Supplementary information:

Capillary flow experiments (Capflex) for thermodynamic and kinetic characterization of protein LLPS at high throughput

Emil G. P. Stender[a], Rasmus K. Norrild[a], Jacob Aunstrup Larsen[a], Henrik Jensen[b] and Alexander K. Buell*[a]

1. Experimental Procedures

Materials

pET30M-2 plasmids encoding His_tag-GST-TEV_site-Ddx4n1 or His_tag-GST-TEV_site-Ddx4n1-YFP (see sequence details below) were donated by Dr. Tim Nott (Oxford University). Ampicillin resistant TEV plasmid encoding MBP–TEV_site–His-tag–S-TEV was donated by Charlotte O'Shea (University of Copenhagen). All constructs where sequenced by GATC (Eurofins, Germany) in order to ensure no point mutations have occurred. Tris, TCEP, NaCl, $CaCl_2$, PEG3000, Imidazole, LB broth, benzonase, ampicillin, kanamycin and reduced glutathione were all purchased from VWR (Denmark). ssDNA as previously described to be partitioned by Ddx4n1 droplets by Nott *et al.*[1] with sequence 5'.TTT TTC CTA GAG AGT AGA GCC TGC TTC GTG G-3' as well as the 5' alexa488 labelled version was synthesized, HPLC purified and lyophilized by TAGCopenhagen (Denmark). The RP_3 peptide was synthesized and HPLC purified by Bachem (Switzerland) and delivered as TFA salt after MALDI-MS quality control. Fluoresbrite® YG Microspheres of calibration grade were purchased from Polysciences Europe GmbH (Germany). All buffer components and materials were dissolved in RNAse and nuclease free milliQ water unless otherwise specified.

Protein expression and Purification

Overnight cultures of *E. coli* BL21 (DE3) carrying the plasmid encoding the MBP–TEV_site–His-tag–S-TEV were inoculated into 1 L LB-Amp media in a 3 L flask and grown at 37°C at 160 rpm shaking. When OD_{600} = 0.8 was reached the expression of the construct was induced by addition of IPTG to a final concentration of 1 mM. The induced cells were incubated over night for 16 h at 20°C at 160 rpm shaking. The cells were harvested by centrifugation at 4°C, 7000 g, 20 min and stored at -20°C until use. The expressed MBP-TEV construct undergoes immediate auto cleavage upon expression. Cells were resuspended in 50 mL 20 mM Tris pH 7.8, 200 mM NaCl, 1% Glycerol at 4°C, and lysed by sonication for 12 x 30 sec on ice. The lysate was centrifuged for 20 min at 20,000g, 4°C, and the supernatant was loaded onto 2 mL Ni-NTA resin equilibrated with 20mM Tris pH 7.5, 200 mM NaCl at 4°C. The resin and supernatant were incubated at 4°C for 1 h under gentle mixing fast enough for the resin not to sediment. The resin was washed with 20 mM Tris pH 7.5, 100 mM NaCl, 20 mM imidazole and the TEV protease was eluted with 8 mL 20mM Tris pH 7.5, 100 mM NaCl, 250 mM imidazole. The eluted TEV protease was dialyzed against 2 L 50 mM Tris pH 7.5, with 100 mM NaCl, 10 mM β-mercaptoethanol, 1 mM EDTA at 4°C using 6 kDa cut-off membrane. Glycerol was added to the protein to a final concentration of 50 % and it was stored at -80°C until use.

Expression of Ddx4n1 constructs was carried out by transforming the pET30M-2 carrying the Ddx4n1 constructs into *E. coli* BL21 (DE3). Overnight cultures of these where inoculated into 4 L of LB-KAN media in 4 3 L flasks and incubated at 37 °C at 160 RPM until an OD_{600} between 0.6 and 0.8 was reached. The expression was then induced by addition of IPTG to a final concentration of 0.5 mM. The temperature was lowered to 20°C and the expression took place overnight for 16 h. The cells were harvested by centrifugation at 7000 g, 4°C, 20 min and stored at -20 °C until use. Cells from 4 L culture were resuspended in 120 mL 50 mM Tris pH 8.0, 500 mM NaCl, 5 mM DTT on ice and 16 µL benzonase was added to remove DNA. The cells were lysed by sonication for 12 x 30 sec on ice, centrifuged (20,000g, 4°C, 20 min) and the supernatant was loaded onto 20 mL Pierce Superflow GST-agarose equilibrated with

50 mM Tris, 500 mM NaCl, pH 8.0. The resin was incubated under gentle mixing for 30 min at 4°C. The bound protein was washed with 50 mM Tris, 500 mM NaCl, pH 8.0 and eluted with 60 mL 50 mM Tris, 500 mM NaCl, pH 8.0 containing 10 mM reduced glutathione, all at 4°C. The eluted protein was stored in the fridge over night. EDTA and DTT were added to the eluted protein to a final concentration of 1 and 2 mM respectively. 3 mL of the purified TEV protease was added and the sample was incubated at ambient temperature for 3 h under gentle mixing. The cleaved Ddx4n1 constructs were purified by Reverse IMAC by loading the sample onto 10 mL Ni-NTA resin equilibrated with 25 mM Tris, 250 mM NaCl, 20 mM Imidazole. The Ni-NTA resin binds both the TEV protease and the cleaved GST tag. The resin was incubated under gentle mixing for 30 min and the flow through was collected, concentrated to 1 mL using 10 kDa cut-off spin filters. 1 mL of the concentrated protein was loaded onto a superdex 75 16/60 column (GE healthcare) equilibrated with 20 mM Tris pH 8.0, 300 mM NaCl, 5 mM TCEP and the protein was eluted at a flow rate of 1 mL/min at 7°C. Protein purity was assesed by SDS-PAGE and MALDI-TOF operating in linear positive mode (Ultraflex II, Bruker Daltonics). Protein concentrations were assessed by measurement of the absorption at 280 nm and the concentrations calculated using theoretical extinction coefficients predicted by ProtParam[2] (Expasy, Switzerland). The verification of the absence of DNA and of the reproducibility of cloud points between batches was performed using a multichannel spectrophotometer/fluorimeter with thermal control (Probedrum, ProbationLabs, Sweden). The purified Ddx4n1 and Ddx4n1YFP proteins were concentrated to 500 and 320 µM respectively, aliquoted and stored at -80°C until use. Total protein yields from 4 L culture was up to 11 mg of protein.

LLPS analysis with FIDA 1 by capillary flow experiments (Capflex).

For Ddx4n1 LLPS experiments, the sample chamber containing the glass vials with 30 µL sample was kept at a temperature above the cloud point of the respective set of solution conditions. PEG3000 was added to 50 µM Ddx4n1 in 20 mM Tris pH 8.0, 100 mM NaCl, 5 mM TCEP to a final concentration of 0 - 7 %. The influence of $CaCl_2$ was investigated at a concentration of 100 µM Ddx4n1 and a $CaCl_2$ concentration between 0 – 10 mM. Influence of protein concentration was investigated at a Ddx4n1 concentration between 100 – 163 µM. The influence of ssDNA was investigated at a concentration of 128 µM Ddx4n1 and a ssDNA concentration between 0 and 30 µM, with the addition of the fluorescent Ddx4n1YFP. Ddx4n1-YFP was added to the 500 µM Ddx4n1 stock solution to a final concentration of 200 nM. When the Alexa488 labelled DNA was used as indicator it was at a Ddx4n1 concentration of 112 µM, 0-26 µM ssDNA and 0.5 % labelled DNA. Fluoresbrite spheres were diluted 4000 times for the 6 µm spheres and 400,000 times for the 1 µm spheres in 20 mM Tris pH 8.0, 100 mM NaCl prior to Capflex analysis. For all samples, a capillary of inner diameter of 75 µm and a length of 1 m was used.

The following set of experimental parameters was used for all samples (Table S1)

Table S1. Experimental parameters for Capflex analysis on the FIDA 1 instrument. Tray 1 and 2 were maintained at 50°C and the capillary chamber was maintained at 20°C

Tray	Vial	Pressure (mbar)	Time (s)	Outlet	Measure	Comment
2	1	3500	45	Variable	no	1 M NaOH wash
2	2	3500	60	Variable	no	miliQ wash
1	48	3500	60	Variable	no	1 % Tween coat
1	Indicator	3500	40	Variable	no	Buffer wash
1	Analyte	200	540	Variable	yes	Sample application

For the RP_3 peptide the cloud point is above the maximum temperature reachable by the FIDA 1 instrument. Hence, the samples were mixed immediately prior to injection. An RP_3 concentration of 184 µM and a DNA concentration of 3.3 - 40 µM

in 10 mM Tris pH 8.0, 50 mM NaCl was used for the analysis. All experiments were carried out with 0.17% labelled DNA. The capillary was coated using HS-coating (FIDAbio, Denmark) in order to avoid peptide interactions with the capillary surface.

Automated peak and baseline analysis

Baseline and peak height determination was carried out with a python script running in Jupyter 6.1.4 (available here: DOI 10.11583/DTU.14223116) with a peak threshold of 0.2 from the baseline. The start of the signal baseline was defined as the top line of a sigmoid fit (>99%) to the time dependent fluorescence trace from the capillary. Prior to fitting the model, this line was smoothed by removing signal larger than + 10 % of the expected signal predicted by the standard curve and then applying a median filter with a windows size of 31 data points. The baseline fluorescence was then calculated as the lower 5% quantile of this line. The baseline fluorescence intensity was converted into a protein or DNA concentration by running standard samples of known concentration that had not undergone LLPS.

Affinity and complex size determination using FIDA 1

Affinity of Ddx4n1YFP for ssDNA was determined by FIDA analysis.[3] 400 nM Ddx4n1YFP in 20 mM Tris pH 8.0, 100 mM NaCl, 5 mM TCEP was used as indicator, more than 2 orders of magnitude bellow the lower critical concentration of LLPS. This binding affinity measurement was performed with a constant, low protein concentration that was titrated with increasing concentrations of DNA, because the inverse experiment suffers from complications when high protein concentrations are reached that undergo LLPS. ssDNA concentration of 0 - 284 µM was added to both indicator and analyte. All samples were measured in triplicates.
The following set of instrumental parameters was used, as detailed in Table S2.

Table S2. Method for FIDA analyses for affinity determination of polypeptides and LLPS inducing compounds. Tray 1 and 2 was maintained at 20°C the capillary chamber was maintained at 20°C

Tray	Vial	Pressure (mbar)	Time (s)	Outlet	Measure	Comment
2	1	3500	45	Variable	no	1 M NaOH wash
2	2	3500	60	Variable	no	miliQ wash
1	48	3500	60	Variable	no	1 % Tween coat
1	46	3500	40	Variable	no	Buffer wash
1	Analyte	3500	20	Variable	no	Analyte capillary fill
1	Indicator	50	10	Variable	no	Indicator plug inject
1	Analyte	400	180	Variable	yes	Mobilize and measure

Apparent hydrodynamic radius (R_h) was determined by analyzing the resulting taylorgrams with the FIDA software suite (FIDAbio, Denmark)
A 1 to 1 (Eq 1) or 1 to 2 (Eq 2) binding model was fitted to the resulting data
Eq 1

$$R_h = \frac{\left(1 + \frac{1}{K_d} * [analyte]\right)}{\left({R_{h_{unbound}}}^{-1} - {R_{h_{bound}}}^{-1}\right) + \left(1 + \frac{1}{K_d} * [analyte]\right) * {R_{h_{bound}}}^{-1}}$$

Were R_h is the apparent hydrodynamic radius of the sample, K_d the dissociation constant, $R_{h\_unbound}$ and R_{h_bound} the apparent hydrodynamic radii of the free and complexed form of the indicator.[4]

For RP_3 lDNA was used as indicator at a concentration of 83 nM and RP_3 peptide was added at a concentration of 0 – 358 µM in 10 mM Tris-HCl and 50 mM NaCl.
A two site model was fitted to the data (Eq 2)
Eq 2

$$R_h = \frac{\left(1 + \left(\frac{1}{K_d}\right)^2 * [analyte]^2\right)}{\left({R_{h_{unbound}}}^{-1} - {R_{h_{bound}}}^{-1}\right) + \left(1 + \left(\frac{1}{K_d}\right)^2 * [analyte]^2\right) * {R_{h_{bound}}}^{-1}}$$

Both models were fitted using Origin Pro 2019 software suite (Originlabs, USA). The model with two binding sites assumes full cooperativity (Hill exponent 2) and does not include the molecular species with only one ligand bound. The reason for this simplification is that the experimental data only provides well-defined sizes for the species with 0 and all (2) ligands bound. Inclusion of a species with 1 ligand bound and a separate hydrodynamic radius would lead to overfitting. The association constant for the reaction is written as a square, according to $(K_a)^2 = [IA_2]/([I][A]^2)$, where [I] is the concentration of indicator (Ddx4n1-YFP in case 1 and labelled DNA in case 2) and [A] is the concentration of analyte (DNA in case 1 and RP3 in case 2). In the main manuscript, we quote the value of K_a, which provides a more intuitive measure for the concentration at which binding occurs than the formal overall binding affinity $(K_a)^2$. The model can be easily modified to make it suitable for even higher stoichiometries. For a 1:3 stoichiometry, the exponents "2" in Eq. 2 need to be replaced by "3", etc.
Figure S9 shows a comparison of fits with the 1:1, 1:2 and 1:3 models to the data for both Ddx4n1-ssDNA and RP_3-ssDNA.

Capflex measurements of droplet formation kinetics

For the measurements of initial droplet formation kinetics 50 µM Ddx4n1 with 2 – 4 % PEG3000 in 20 mM Tris pH 8.0, 100 mM NaCl, 5 mM TCEP were incubated in the sample trays at 55°C, which is above the cloud point. The capillary chamber was kept at 20°C a standard capillary with inner diameter of 75 µm and a length of 1 m was used. The following set of instrument parameters were used (Table S3)

Table S3. Experimental parameters for Capflex analysis of kinetics of droplet formation on the FIDA 1 instrument. Tray 1 and 2 were maintained at 55°C and the capillary chamber was maintained at 20°C

Tray	Vial	Pressure (mbar)	Time (s)	Outlet	Measure	Comment
2	1	3500	45	Variable	no	1 M NaOH wash
2	2	3500	60	Variable	no	miliQ wash
1	48	3500	60	Variable	no	1 % Tween coat
1	46	3500	40	Variable	no	Buffer wash
1	Analyte	3500	20	Variable	no	Analyte capillary fill
1	Analyte	300	240	Variable	yes	Kinetics measure

Data analysis was performed using origin Pro 2019 (Originlabs, USA), using the asymmetric least squares smoothing baseline with a Symmetric factor of 0.001, threshold of 0.005, smoothing factor of 4 and 20 iterations. The validity of the baseline was verified by visual inspection for all graphs. A local maximum more than 1 % different from the baseline is considered a peak and hence a droplet. Averaging peak intensities with a sliding window of 10 peaks then generated overall curves of droplet formation kinetics.

Relative enrichment factor calculation

The relative enrichment of protein to DNA inside droplets was determined in a sample of 112 µM Ddx4n1 and a total DNA concentration of 3.3 µM. Either Ddx4n1YFP or lDNA was used as fluorescent reporter. The peaks and curve were integrated using Origin Pro (Origin Labs, USA). Positive signal more than 0.5 % from the baseline was considered a peak. The Enrichment factor was calculated by taking the sum of the peak integrals and dividing by the total curve integral:

Ratio = SUM(peaks)/(Curve area)

This ratio for both protein and DNA was then divided, according to:

Relative enrichment = Ratio(Protein)/Ratio(ssDNA)

yielding the relative enrichment factor.

Microscopy

Microspopy images were recorded at 40 times magnification using a DIC capable microscope Nikon Eclipse Ti2 (RAMCON, Denmark) at the DTU bio-imaging core facility using GFP filters for detection of YFP or alexa488 fluorescence. The exposure time was adjusted for each image to ensure the highest possible amount of droplets detected. 500 nM Ddx4n1YFP or 250 nM lDNA was used as reporter in all samples. Image analysis was carried out using ImageJ (NIH, USA)

Cuvette-based spectroscopy and scattering experiments

Cloud points and the influence of additives on Ddx4n1 and Ddx4n1YFP fluorescence was investigated using a multichannel spectrophotometer equipped with a thermal control and IR temperature measurement, the ProbeDrum (ProbationLabs, Lund, Sweden). Samples of 50 µL were scanned from 12-60°C in a high precision Cell Quartz glass cuvette with 3x3 mm light path (Hellma Analytics, Germany) while measuring the absorbance at 240-700 nm, fluorescence at 240-700 nm with excitation at 280 nm and 509 nm as well as static light scattering at 90° with a laser of 638 nm for all time points. The temperature scan rate was 2°C per minute and measurements were taken every 5 s. Initial data analysis was carried out using PDviewer (ProbationLabs, Sweden) and the data were visualized using Origin Pro 2019 (OriginLabs, USA).

From relative peak intensities to relative droplet sizes

In order to be able to translate a relative Capflex peak intensity distribution into a relative droplet size distribution, the non-uniform flow velocity across the capillary cross-section needs to be considered. Droplets that cross the detection area of the capillary with different flow rates will reside for different time periods in the detection area and hence the integrated signal intensity differs. In addition to the effects of the parabolic flow profile of Poisseuille flow, flow focusing might also need to be taken into account. Furthermore, potential droplet deformation in the shear field of the capillary flow should be considered. Below, we discuss these effects separately.

Radial particle distribution

Two types of particle focusing mechanisms need to be considered in the FIDA system: Dean flow and radial migration. Dean flow is a concern when the dean number, k (Eq 3), is not significantly smaller than one.[5]
Eq 3

$$k = \sqrt{\frac{H}{2R}}\, Re \approx \sqrt{\frac{10^{-4}}{2 \cdot \frac{1}{2} 10^{-2} m}}\, 1 = 10^{-1}$$

Where H is the capillary diameter, Re is the Reynolds number of the flow and R is the turn radius of the capillary. Hence, Dean flow can be neglected in the FIDA 1 setup.
Dino Di Carlo has provided some general design rules for particle focusing microfluidic systems[5], which will be utilized to generalize whether radial migration is a concern in this system. The conditions explored here are the most advantageous

conditions for particle focusing in this study. The Hagen-Poiseuille equation can be used to predict the velocity of the fluid in a capillary (Eq 4)[6]
Eq 4

$$U_m = \frac{\Delta P\, D^2}{4\,\mu\, L} = \frac{10^5\ 10^{-8}}{8\ 10^{-3}}\frac{m}{s} \approx 10^{-1}\frac{m}{s}$$

Where U_m is maximum velocity, ΔP is the pressure, D is the capillary diameter, μ is dynamic viscosity (approximated to that of pure water) and L is capillary length. The length necessary for significant focusing of general particles/droplets is expressed as (Eq 5)
Eq 5

$$L_f = \frac{\pi\,\mu\, H^2}{\rho\, U_m\, a^2\, f_e} = \frac{\pi\ 10^{-3}10^{-8}}{10^3\ \cdot 10^{-1}\cdot 10^{-12}\ \cdot 0.05}\ m \approx 60\ \frac{10^{-11}}{10^{-10}}m = \ 6\ m$$

Where H is smallest capillary dimension (diameter), ρ is fluid density (approximated to that of pure water), a is particle radius and f_e is a lift force factor usually between 0.02 and 0.05. Since significant radial migration is only obtained after several capillary lengths in the highest velocity case, it is safe to assume that particles in this experiment are randomly distributed throughout the cross-section, assuming random nucleation of droplets.

Signal intensity distribution from randomly distributed particles
Assuming a random particle distribution across the cross-section of the capillary, it is possible to evaluate a signal profile of a monodisperse particle solution. Particle flux throughout the radius must be proportional to flow velocity at any radius multiplied by the probability of finding a particle at any radius. The probability expression must be proportional to the circumference and hence linearly proportional to the radius. Hence particle flux $\propto \left(1-\frac{r}{R}\right)^2 \cdot r$:

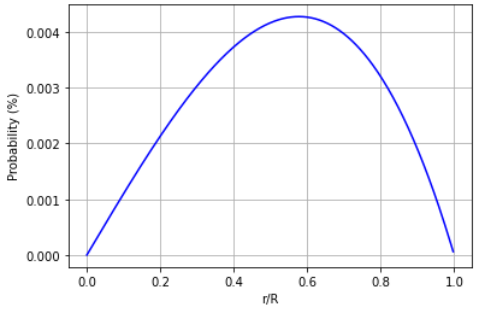

Figure S1. Particle flux as a function of radius from center of the capillary, assuming random particle distribution.

This distribution has been numerically correlated with signal intensity, which is related to the reciprocal particle velocity, and the resulting signal distribution has then been fitted to the calibration data acquired with the 1 μm polystyrene monodisperse spheres:

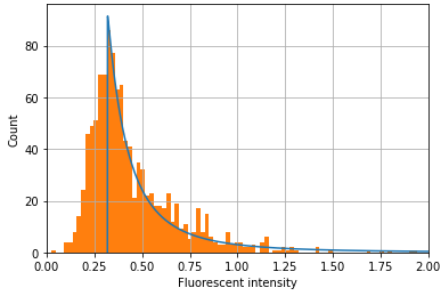

Figure S2. Expected signal distribution (blue line) overlaid the 1 μm polystyrene sphere calibration data (histogram).
The model reproduces the experimentally observed tail at higher signal intensities well, supporting the assumption of random particle distribution described above. A number of signal intensities of significantly lower than the expected minimal signal (corresponding to particles in the center of the capillary traveling at the fastest flow rate) are likely to be explained by the intrinsic variability of the absolute fluorescence intensity of the particles (see supplementary figure S4).

Shear stress and droplet deformation
LLPS droplets are likely to undergo some degree of deformation, when exposed to the shear stress of a laminar flow. The maximum expected shear stress during these experiments is at the inner wall of the capillary (Eq 6)
Eq 6

$$\tau_w = \gamma_w \cdot \mu = \frac{8U_m}{D}\mu \approx \frac{2\cdot 10^{-1}}{10^{-4}}10^{-3}Pa = 2\ Pa$$

Which is similar to the stress which has been found to deform and induce aggregation in FUS droplets.[7] However, in these experiments, a channel geometry optimized for droplet deformation was used (perpendicular channels).

Quantifying the degree and effect of shear stress on droplet deformation and potential breakup is difficult, as very little is known about the physical characteristics of such droplets (surface tension, viscosity) and their dependence on solution conditions.
While droplet deformation will impact their flow through the capillary, it is unlikely to affect the detection and quantification of droplets. The total fluorescence intensity emitted by a droplet is likely to be unaffected by its shape, as well as by a potential shear-mediated liquid-to-solid transition, as the fluorophore quantity of each droplet is maintained throughout such a transition. It should be noted that there is currently no evidence that the protein system used in the present study (Ddx4n1) is able to undergo such a shear-mediated liquid-to-solid-transition.
At very large shear forces, droplet breakup can influence the quantification of relative droplet size distributions. However, most Capflex experiments were performed at moderate flow rates and no evidence for droplet breakup was observed under any conditions.

Amino acid sequences

TEV protease:

MFNLQEPYFTWPLIAADGGYAFKYENGKYDIKDVGVDNAGAKAGLTFLVDLIKNKHMNADTDYSIAEAAFNKGETAMTINGP
WAWSNIDTSKVNYGVTVLPTFKGQPSKPFVGVLSAGINAASPNKELAKEFLENYLLTDEGLEAVNKDKPLGAVALKSYEEELA
KDPRIAATMENAQKGEIMPNIPQMSAFWYAVRTAVINAASGRQTVDEALKDAQTNSSSNNNNNNNNNNLGIEGRGENLYFQ
GHHHHHHHGESLFKGPRDYNPISSTICHLTNESDGHTTSLYGIGFGPFIITNKHLFRRNNGTLLVQSLHGVFKVKNTTTLQQHL
IDGRDMIIIRMPKDFPPFPQKLKFREPQREERICLVTTNFQTKSMSSMVSDTSCTFPSSDGIFWKHWIQTKDGQCGSPLVSTR
DGFIVGIHSASNFTNTNNYFTSVPKNFMELLTNQEAQQWVSGWRLNADSVLWGGHKVFMVKPEEPFQPVKEATQLMNRRR
RR

MBPTEVsiteHISTEVprotease

GST-TEVsite-Ddx4n1:

HHHHHHMSPILGYWKIKGLVQPTRLLLEYLEEKYEEHLYERDEGDKWRNKKFELGLEFPNLPYYIDGDVKLTQSMAIIRYIADK
HNMLGGCPKERAEISMLEGAVLDIRYGVSRIAYSKDFETLKVDFLSKLPEMLKMFEDRLCHKTYLNGDHVTHPDFMLYDALD
VVLYMDPMCLDAFPKLVCFKKRIEAIPQIDKYLKSSKYIAWPLQGWQATFGGGDHPPKSDLVPRGSPGIHRDENLYFQGGAM
GSMGDEDWEAEINPHMSSYVPIFEKDRYSGENGDNFNRTPASSSEMDDGPSRRDHFMKSGFASGRNFGNRDAGECNKRD
NTSTMGGFGVGKSFGNRGFSNSRFEDGDSSGFWRESSNDCEDNPTRNRGFSKRGGYRDGNNSEASGPYRRGGRGSFR
GCRGGFGLGSPNNDLDPDECMQRTGGLFGSRRPVLSGTGNGDTSQSRSGSGSERGGYKGLNEEVITGSGKNSWKSEAE
GGES

HisGSTTEVsiteDdx4n1

His_tag-GST-TEV_site-Ddx4n1-YFP:

HHHHHHMSPILGYWKIKGLVQPTRLLLEYLEEKYEEHLYERDEGDKWRNKKFELGLEFPNLPYYIDGDVKLTQSMAIIRYIADK
HNMLGGCPKERAEISMLEGAVLDIRYGVSRIAYSKDFETLKVDFLSKLPEMLKMFEDRLCHKTYLNGDHVTHPDFMLYDALD
VVLYMDPMCLDAFPKLVCFKKRIEAIPQIDKYLKSSKYIAWPLQGWQATFGGGDHPPKSDLVPRGSPGIHRDENLYFQGGAM
GSNMGDEDWEAEINPHMSSYVPIFEKDRYSGENGDNFNRTPASSSEMDDGPSRRDHFMKSGFASGRNFGNRDAGECNKR
DNTSTMGGFGVGKSFGNRGFSNSRFEDGDSSGFWRESSNDCEDNPTRNRGFSKRGGYRDGNNSEASGPYRRGGRGSF
RGCRGGFGLGSPNNDLDPDECMQRTGGLFGSRRPVLSGTGNGDTSQSRSGSGSERGGYKGLNEEVITGSGKNSWKSEA
EGGESSDTQGPKVTLQMVSKGEELFTGVVPILVELDGDVNGHKFSVSGEGEGDATYGKLTLKFICTTGKLPVPWPTLVTTFG
YGLMCFARYPDHMKQHDFFKSAMPEGYVQERTIFFKDDGNYKTRAEVKFEGDTLVNRIELKGIDFKEDGNILGHKLEYNYNS
HNVYIMADKQKNGIKVNFKIRHNIEDGSVQLADHYQQNTPIGDGPVLLPDNHYLSYQSKLSKDPNEKRDHMVLLEFVTAAGIT

HisGSTTEVsiteDdx4n1YFP

2. Results and Discussion

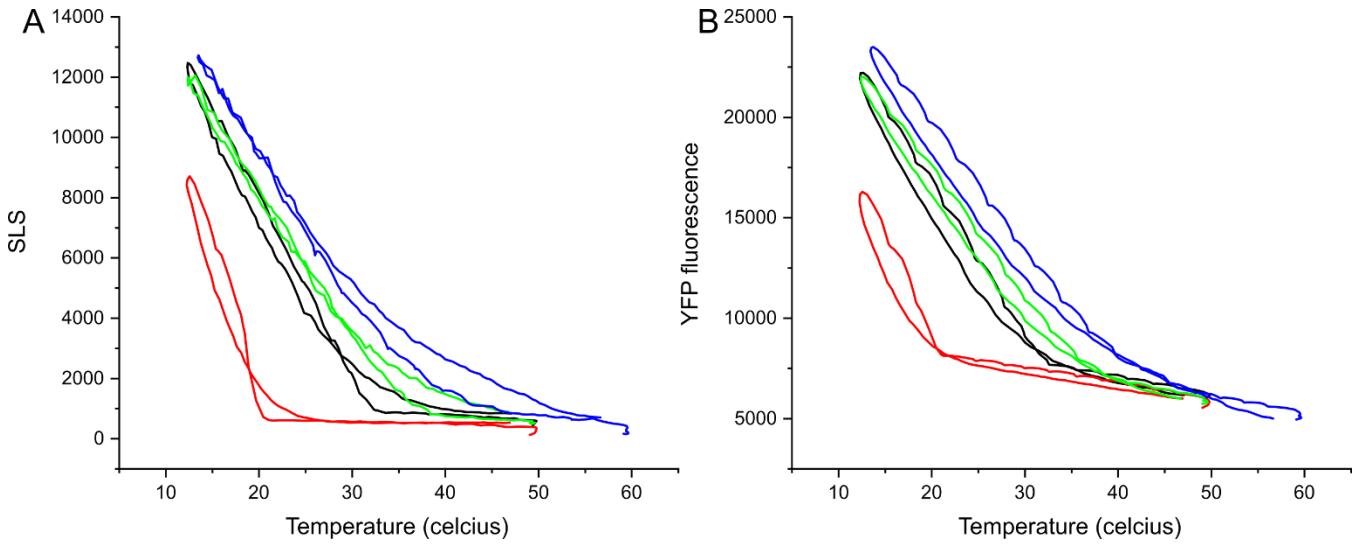

Figure S3. Cloud point determination, LLPS reversibility and the influence of PEG3000. A) Thermal ramp of 50 µM Ddx4n1 and 0-4 % PEG3000 monitored by static light scattering intensity. B) Thermal ramp of 50 µM Ddx4n1 and 0-4 % PEG3000 monitored by YFP flourescence 0 % (Red), 2 % (black), 3 % (green), 4 % (blue).

The cloud point increases as a function of PEG3000 concentration and the process is reversible. Increase in YFP fluorescence upon passing the cloud point is due to the Probedrum instrument being without a detector filter in order to be able to record multiple channels at once, which leads to the detection of scattered excitation light. When no LLPS is present in the samples at 50°C there is no difference in YFP fluorescence in the samples with different PEG concentrations, indicating, that there is no quenching of YFP signal by addition of PEG3000.

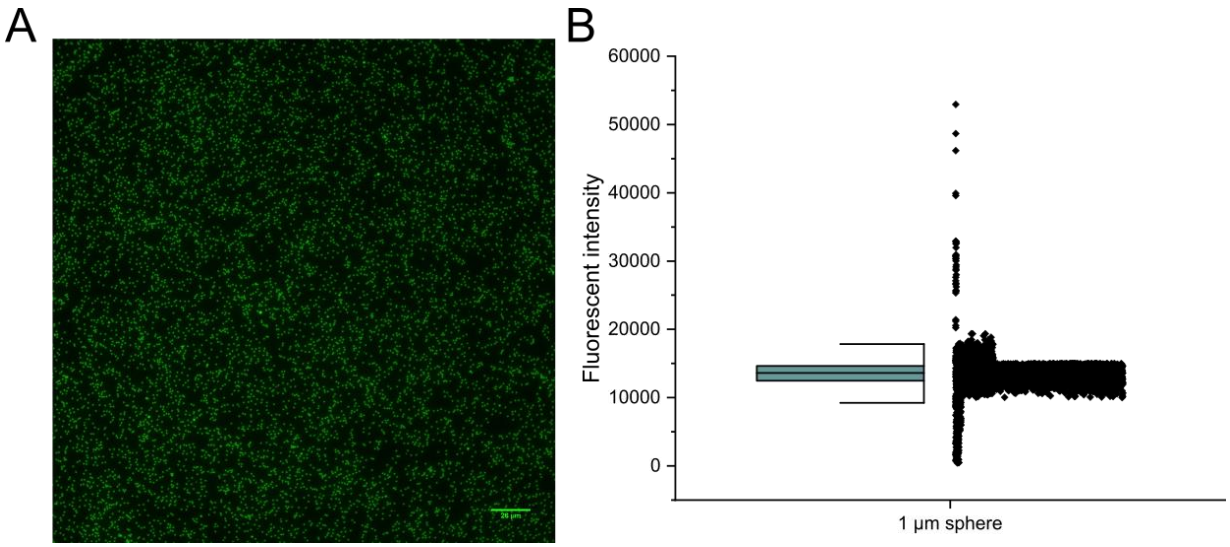

Figure S4. Fluorescence microscopy image of the 1 µm polystyrene spheres. A) fluorescence microscopy image. B) fluorescence intensity distribution from the microscopy image.

The fluorescence intensity distribution of the 1 µm calibration spheres is narrow indicating that spheres have a homogeneous fluorescence intensity. However, a significant number of particles with lower intensity are observed, potentially explaining the tail of the Capflex peak intensity distribution when these calibration spheres are measured (see above).

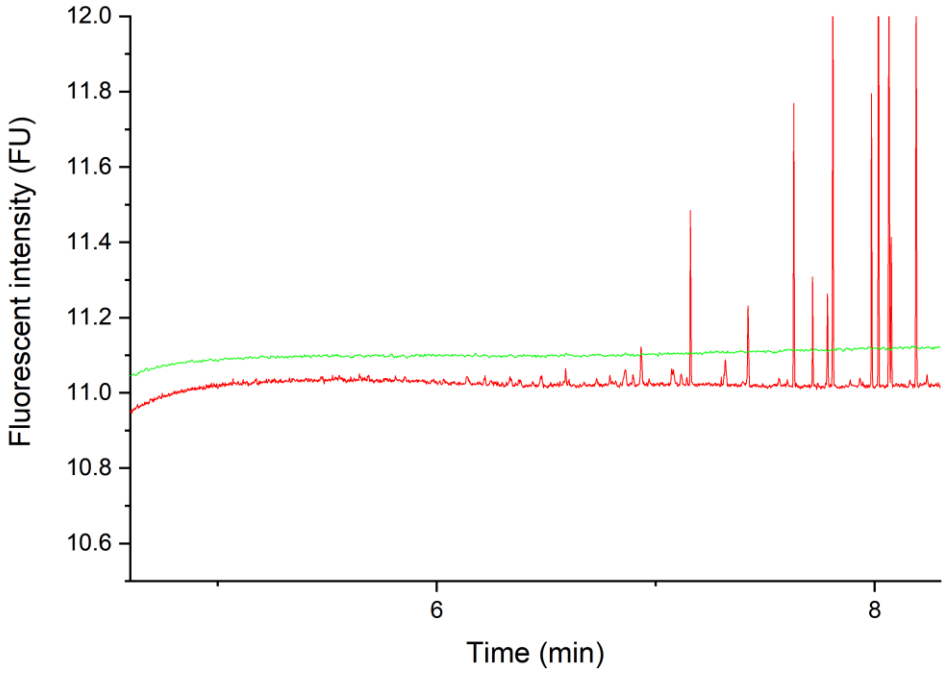

Figure S5. Capflex of 112 µM Ddx4n1 with 6 µM total ssDNA, 30 nM lDNA (red) and in the absence of Ddx4n1, with 4 µM total ssDNA, 20 nM lDNA (green)

The ssDNA is incapable of undergoing LLPS on its own and therefore the green line in Figure S3 corresponds to the free signal of 4 µM ssDNA and gives an impression of the very low noise level when no LLPS has occurred. The red line corresponds to 112 µM Ddx4 with 6 µM total ssDNA. The baseline is significantly more noisy compared to the 4 µM ssDNA demonstrating that very small droplets are likely present, that cannot easily be distinguished from baseline noise.

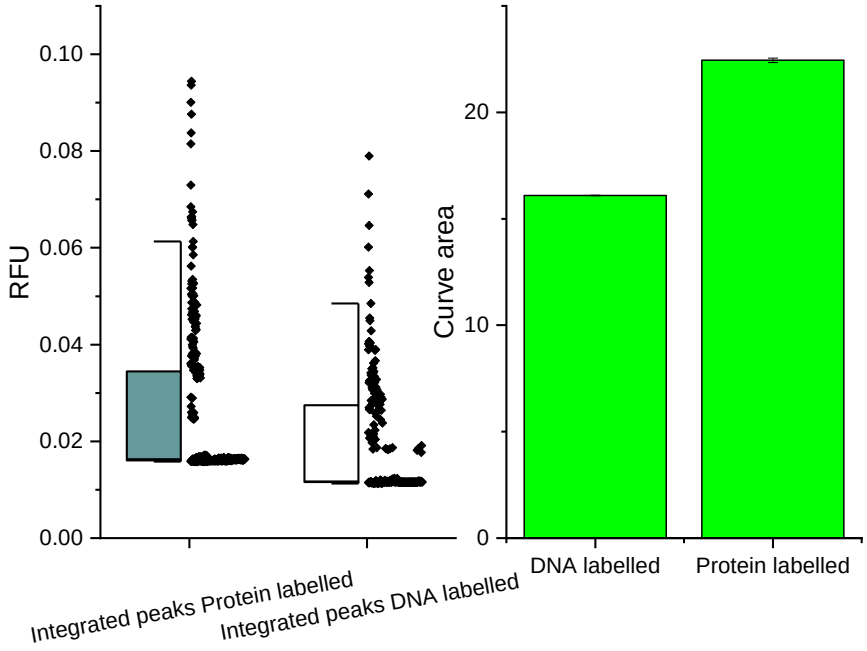

Figure S6. Data used to calculate the relative partitioning of ssDNA and protein. Integrated signal spikes for 3 data sets (left) integrated baseline the error bar is the standard deviation of a triplicate (right).

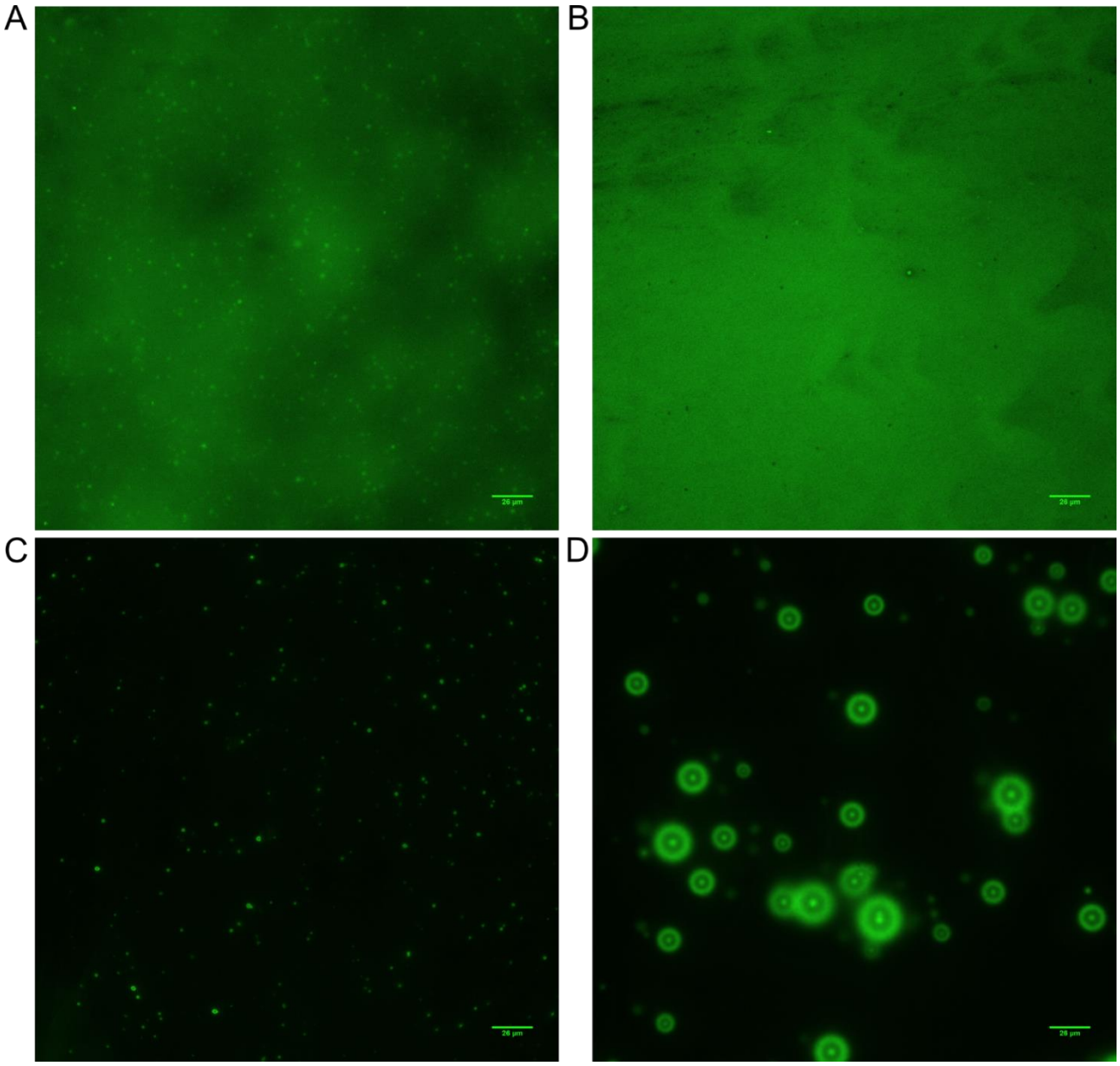

Figure S7. Fluorescence microscopy image of RP_3 peptide with ssDNA and 500 nM lDNA. A) 184 µM RP_3 10 µM DNA. B) 46 µM RP_3 70 µM DNA. C) 46 µM RP_3 10 µM DNA. D) 46 µM RP_3 10 µM DNA after 20 min incubation

When the peptide is in excess compared to DNA only little LLPS occurs and the majority of the DNA is found in the light phase. When DNA is present in large excess, no LLPS occurs. At the optimal conditions, the majority of the DNA is found in the dense phase and these droplets grow significantly with time and form core shell structures, which has been observed previously by Banerjee *et al.*[8]

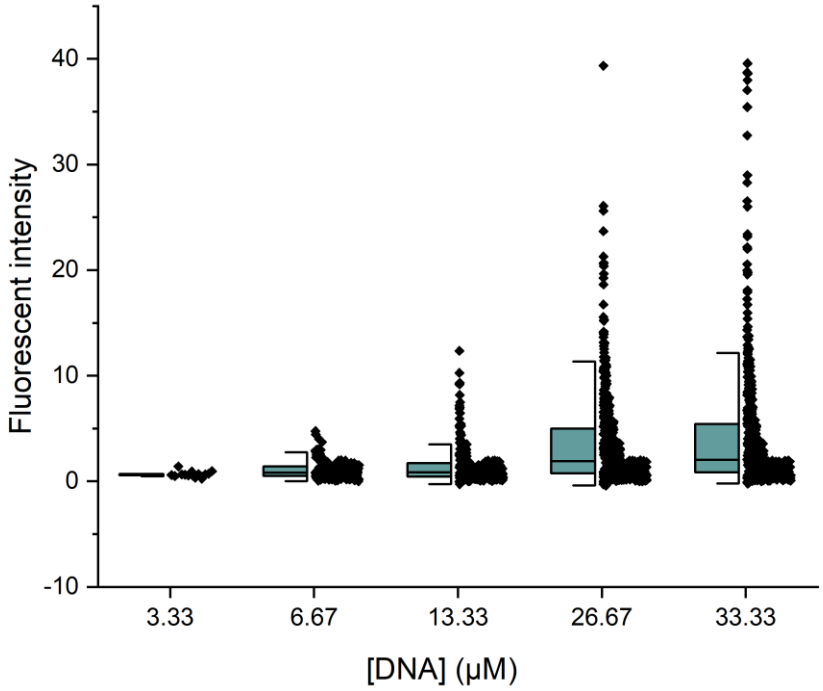

Figure S8. Droplet size distribution of RP_3/ssDNA coacervation. The droplet intensity is normalized to the baseline to compensate for increased presence of lDNA.

Analysis of Ddx4n1 and RP_3 binding to ssDNA.

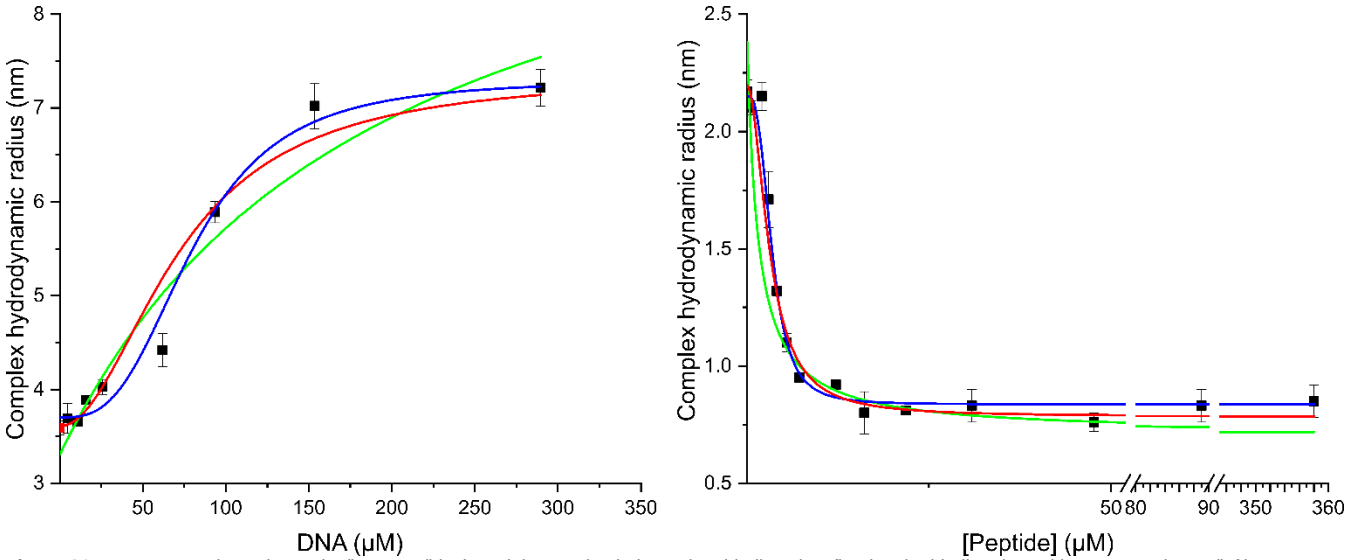

Figure S9: A one to one (green), two (red) or tree (blue) model assuming independent binding sites fitted to the binding data with ssDNA. Ddx4n1 (left) RP_3 peptide (right

A one to one model fits both datasets poorly. As there is a large difference in the relative size of the binding partners in both cases, a multivalent model seems reasonable to assume. There is no significant difference between the dissociation constant yielded by the one to two and the one to tree binding models, and hence we applied the 1:2 binding model in both cases.

References

[1] T. J. Nott, E. Petsalaki, P. Farber, D. Jervis, E. Fussner, A. Plochowietz, T. D. Craggs, D. P. Bazett-Jones, T. Pawson, J. D. Forman-Kay, A. J. Baldwin, *Mol. Cell* **2015**, *57*, 936–947.

[2] E. Gasteiger, C. Hoogland, A. Gattiker, S. Duvaud, M. R. Wilkins, R. D. Appel, A. Bairoch, *Proteomics Protoc. Handb.* **2005**, 571–607.

[3] H. Jensen, J. Østergaard, *J. Am. Chem. Soc.* **2010**, *132*, 4070–4071.

[4] M. E. Pedersen, J. Østergaard, H. Jensen, *ACS Omega* **2020**, *5*, 10519–10524.

[5] D. Di Carlo, *Lab Chip* **2009**, *9*, 3038–3046.

[6] A. Ostadfar, *Fluid Mechanics and Biofluids Principles*, **2016**.

[7] Y. Shen, F. S. Ruggeri, D. Vigolo, A. Kamada, S. Qamar, A. Levin, C. Iserman, S. Alberti, P. S. George-Hyslop, T. P. J. Knowles, *Nat. Nanotechnol.* **2020**, *15*, 841–847.

[8] P. R. Banerjee, A. N. Milin, M. M. Moosa, P. L. Onuchic, A. A. Deniz, *Angew. Chemie - Int. Ed.* **2017**, *56*, 11354–11359.